Structure of pressure-induced amorphous form of SnI_4 at high pressure

Ayako Ohmura,* Kyoko Sato, and Nozomu Hamaya
Graduate School of Humanities and Sciences, Ochanomizu University, 2-1-1 Ohtsuka, Bunkyo-ku, Tokyo 112-8610, Japan

Maiko Isshiki† and Yasuo Ohishi
Japan Synchrotron Radiation Research Institute (JASRI), 1-1-1 Kouto, Sayo-cho, Sayo-gun, Hyogo 679-5198, Japan
(Received 7 January 2009; revised manuscript received 11 June 2009; published 20 August 2009)

The structure of pressure-induced amorphous form of SnI_4 has been studied by synchrotron x-ray diffraction measurements using diamond-anvil cell. The structure factor, the reduced radial distribution function, and the density were obtained between 25 and 55 GPa. Comparison of measured structure factor with that calculated for a randomly oriented dimerized molecules model shows no similarity between them. Experimentally obtained radial distribution function provides clear evidence for the absence of both distances between tin and iodine atoms and between iodine atoms within the SnI_4 tetrahedral molecule. Characteristic features of the structure factor for amorphous SnI_4 show a marked resemblance to those for elemental metallic glasses which are successfully reproduced by a model of dense random packing of equal-sized spheres. Indeed, various quantities such as positions of peaks in measured structure factors and in experimental radial distribution functions, the coordination number are in precise agreement with those derived from the dense random-packing model. We conclude that the structure of the high-pressure amorphous form of SnI_4 is the relatively rigid packing of tetrahedra composed of iodine and substitutional tin atoms.

DOI: 10.1103/PhysRevB.80.054201 PACS number(s): 62.50.−p, 81.40.Vw, 61.05.cf, 61.43.Dq

I. INTRODUCTION

Since the discovery of the high-density amorphous ice by Mishima *et al.*,[1] pressure-induced amorphization has been observed in various systems.[2–10] In particular, the finding of polymorphism in the tetrahedral glassy and liquid forms such as H_2O, Si, and P has attracted extensive experimental and theoretical interest.[11–17] Tin tetraiodide SnI_4 is also inferred to show amorphous polymorphism under pressure from the fact that the position of the first peak of an amorphous form exhibits pressure hysteresis accompanied by discontinuous jumps.[18] Such structural variation seems likely to be a transition from high-density to low-density amorphous SnI_4 (denoted as HDA and LDA, respectively). Although there have been a variety of experimental studies on SnI_4 under pressure,[18–27] the structure of pressure-induced amorphous forms of SnI_4 is still controversial.

The tetrahedral SnI_4 molecule has the tin atom at the center and covalently bonded four iodine atoms at the corners. The molecules are weakly bonded by van der Waals force and ordered into a cubic lattice with space group $Pa\bar{3}$ with eight molecules in a unit cell at 1 atm and room temperature [denoted as crystalline phase I (CP-I)]. The metallic, high-pressure amorphous form of SnI_4 is induced by the application of pressure to CP-I at ~10 GPa (Ref. 20) and recrystallizes to a nonmolecular crystalline phase III (CP-III) at 61 GPa.[18] The structure of CP-III is suggested to be analogous to a substitutional binary alloy in which the tin and iodine atoms are randomly distributed on the fcc lattice sites.[26] When CP-III is decompressed, the high-pressure amorphous form reappears below 30 GPa with a large pressure hysteresis. A change to the low-pressure amorphous form occurs at 1 GPa and the original crystalline phase CP-I recovers at 0.4 GPa. Thus the structure of the high-pressure amorphous SnI_4 is quite interesting in that it is formed in the intermediate state between the molecular and the nonmolecular crystalline structures.

Previous experimental studies proposed different structure models for the high-pressure amorphous SnI_4: (1) random distribution of dimerized SnI_4 molecules from Raman-scattering study,[21] (2) polymerization of randomly oriented molecules from Mössbauer spectroscopy,[22] (3) random network of deformed tetrahedral units from x-ray absorption fine structure spectroscopy (denoted as XAFS) measurement,[24] and (4) nonmolecular disordered structure from our previous x-ray diffraction measurement.[26] In this paper, we show that the amorphization in SnI_4 is accompanied by molecular dissociation and that the structure of its high-pressure amorphous form exhibits remarkable similarities with metallic glasses such as Ni and Fe.

The primary purpose of the present study is to experimentally show the microscopic structure of high-pressure amorphous SnI_4 and its evolution with pressure. We performed synchrotron x-ray diffraction measurements under high pressure using a diamond-anvil cell (DAC) and an imaging plate as a detector. Such structural information is crucial to understand not only the HDA-LDA transition but also various novel phenomena observed in amorphous SnI_4 such as molecular dissociation, metallization, and superconductivity. For instance, the superconducting transition first occurs at 35 GPa at $T=1.32$ K in the amorphous form.[25] The transition temperature increases to 1.96 K at 64 GPa with increasing pressure and then begins to decrease in the crystalline phase III. Part of the present work has been published elsewhere.[27]

II. EXPERIMENT

Polycrystalline SnI_4 of 99.9% purity purchased from Kojundo Chem. Co. was ground into a fine powder. A powder sample was placed into a hole 120 μm diameter drilled in

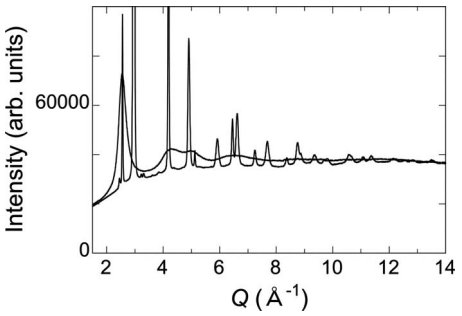

FIG. 1. Diffraction patterns of SnI_4 in high-pressure amorphous form at 55 GPa and in crystalline phase III at 65 GPa.

the rhenium gasket of 50 μm thick and loaded into the modified Mao-Bell-type DAC with 0.3 mm culet anvils. A few ruby chips 5–10 μm diameter were put in the hole together with the sample to determine the pressure by the ruby fluorescence method.[28] No pressure-transmitting medium was used. The pressure variation over the sample irradiated by x rays was measured as less than 1.0 GPa at 65 GPa. The recovered sample has a thickness of 14 μm after compression to 65 GPa. All the sample preparation was made in an argon atmosphere to avoid the reaction of the sample with water in air.

Synchrotron x-ray diffraction measurements were carried out at beamline BL04B2 in SPring-8. Three different runs were conducted above 25 GPa. To cover a wide range of wave number, Q, we used high-energy x rays tuned to 61.53 keV (wavelength $\lambda=0.2015$ Å) with the single-bounce monochromator Si (220) crystal. The incident beam was collimated to 40×40 μm^2. An imaging plate was used as a detector. The acquisition time for each diffraction pattern was either 50 or 100 min and four or two patterns were collected and summed at each pressure to obtain good counting statistics. The intensity of the incident x rays was monitored with an ionization chamber. Diffraction patterns were measured at 54 and 63 GPa in the first run, at 35, 45, 55, and 65 GPa in the second run, at 25, 30, and 68 GPa in the third run on compression, and at 25 GPa on decompression in the second run. The measured diffraction patterns were contaminated by peaks diffracted by x rays with $\lambda/2$. This contamination was estimated to be less than 7% in relative intensity from the measurements of an x-ray standard material of CeO_2. In the present analysis, only the first peak due to $\lambda/2$ located below $Q\leq1.5$ Å^{-1} was removed.

It is particularly important in the intensity analysis to estimate the background intensity. This arises from the incoherent Compton scattering, the thermal diffuse scattering, and the fluorescent scattering from both sample and diamond. The air scattering and the stray x rays around the diffractometer are also included. Figure 1 shows the spectra of both the amorphous state at 55 GPa and crystalline phase III at 65 GPa. The background intensity was estimated from the measured spectrum of crystalline phase III using a curve-fitting program.

Conversion of the raw data to spectra in electron units was carried out as follows. First the observed intensity was normalized to the intensity of the incident x rays. Then, the polarization factor and the absorption due to the sample and the diamond were corrected. The absorption coefficient of the sample was calculated using both the thickness of the recovered gasket after compression and the interpolated density between crystalline phases CP-I and CP-III. After subtracting the background intensity estimated from the spectrum of CP-III, the coherent scattering intensity of the sample in electron units, $I_{eu}^{coh}(Q)$, was obtained by applying the normalization factor calculated by the Krogh-Moe-Norman method.[29,30] Finally, we obtained the Faber-Ziman structure factor $S(Q)$,[31]

$$S(Q)=\frac{I_{eu}^{coh}(Q)-(\langle f^2(Q)\rangle-\langle f(Q)\rangle^2)}{\langle f(Q)\rangle^2}, \tag{1}$$

where $\langle f(Q)\rangle^2$ and $\langle f^2(Q)\rangle$ are, respectively, the square of the average of the atomic-scattering factors and the average of the squared atomic-scattering factors for SnI_4. The reduced radial distribution function $G(r)$ is calculated by sin transform of $S(Q)$,

$$G(r)=4\pi r[\rho(r)-\rho_0]=\frac{2}{\pi}\int_0^{Q_{\max}}Q\cdot\{S(Q)-1\}\sin(Qr)dQ, \tag{2}$$

where r is the atomic distance, $\rho(r)$ and ρ_0 are the atomic number density function and the average atomic number density, respectively. The maximum value of the integral range of Q, $Q_{\max}$, was set at 12 Å^{-1} in this study. No window function was used.

Equation (2) can be reduced to the following expression in a region $0<r<r_{\min}$, where $r_{\min}$ is the shortest atomic distance in the amorphous structure,

$$G(r)=-4\pi\rho_0\cdot r. \tag{3}$$

This equation predicts monotonous decrease in $G(r)$ with increasing r. However, the experimentally obtained $G(r)$ often exhibits unphysical oscillation in the range of $0<r<r_{\min}$. Two major factors causing this oscillation are the estimation error of the normalization factor by Krogh-Moe-Norman method and the termination error in the Fourier transform. Kaplow *et al.*[32] showed how to remove the unphysical oscillation in $G(r)$ and to estimate the atomic number density ρ_0 using the data below $r_{\min}$.[33] They reported that the accuracy of ρ_0 estimated by their method was better than 6%. Adopting their optimization procedure, we improved measured $G(r)$ and obtained ρ_0 using Eq. (3) under high pressure. In this procedure, we chose $r_{\min}$ at the shorter edge of the peak of the nearest-neighbor distance, for example, $r_{\min}=2.34$ Å at 25 GPa.

III. RESULTS

Figure 2 shows the pressure evolution of the structure factor $S(Q)$ measured on compression in this study. A comparison of $S(Q)$ at 54 GPa with that at 55 GPa obtained in different runs demonstrates that the reproducibility of the data is quite good over entire Q values measured. The most dominant features of the measured $S(Q)$ are the intense and sharp first peak and the splitting of the second peak. As the

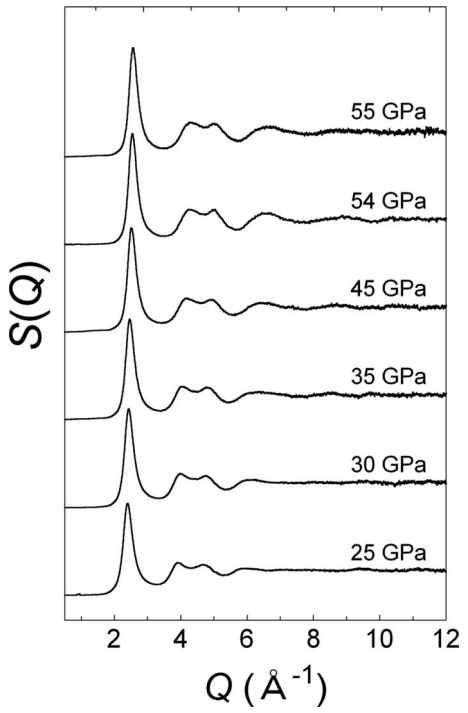

FIG. 2. Structure factor $S(Q)$ for amorphous SnI_4 measured with increasing pressure.

pressure is increased, all peaks shift to larger Q values and the amplitude of oscillation above ~ 5 Å^{-1} gradually develops. These indicate an increase in order of atomic spacing in the amorphous form with increasing density.

Figure 3 shows the reduced radial distribution function

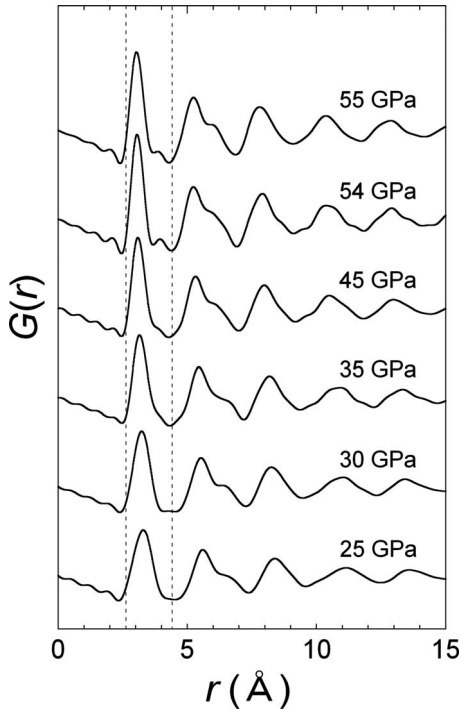

FIG. 3. Reduced radial distribution function $G(r)$ calculated by sin-transform of $S(Q)$ in Fig. 2. Two broken lines denote the intramolecular bond distances of $r_{\text{Sn-I}}=2.65$ Å and $r_{\text{I-I}}=4.33$ Å.

$G(r)$ obtained by sin-transform of $S(Q)$ in Fig. 2. Two broken lines at 2.65 and 4.33 Å denote, respectively, the Sn-I and the I-I atomic distances within the tetrahedral SnI_4 molecule. Apparently the maxima of the first and the second peaks in the measured $G(r)$ do not agree with those intramolecular atomic distances, indicating the absence of the tetrahedral molecules in high-pressure amorphous SnI_4. The strong oscillation above $r\sim 7$ Å is associated with the increased intermediate-range order in the amorphous form. As the pressure is increased, all peaks in $G(r)$ appear to become higher in magnitude and narrower in width. This can be attributed to the development of orders resulting from densification of the amorphous form. It is noted in Fig. 3 that a new order emerges and grows at $r\sim 3.9$ Å with increasing pressure.

Principal structural parameters of amorphous SnI_4 obtained in this study are listed in Table I. Figure 4 illustrates the pressure variation in the atomic distances in amorphous SnI_4 and in the crystalline structures of CP-I and CP-III determined from x-ray diffraction measurements,[18,26] and the distance measured below 22 GPa by XAFS spectroscopy.[24] The intramolecular I-I distance at $r\sim 4.33$ Å vanishes abruptly at ~ 9 GPa, indicating breakdown of the tetrahedral molecules while the slightly elongated Sn-I bond appears and survives to 22 GPa. The most interesting observation in Fig. 4 is the pressure variation in the distance between intermolecular iodine atoms. The first and the second shortest I-I distances in the crystalline phase I become undistinguishable above ~ 10 GPa. On further compression, the I-I and the Sn-I distances merge and make the first shell above 25 GPa. As seen in Fig. 3, the first peak in the measured $G(r)$ at 25 GPa shows no sign of splitting. This distance monotonically decreases down to $r\sim 3.02$ Å at 55 GPa and turns out to be the nearest-neighbor distance in the crystalline phase III without observable discontinuity.

The density of amorphous SnI_4, ρ_m, can be obtained from the estimated average number density ρ_0(Å^{-3}); ρ_m(g cm^{-3}) $=\rho_0\times 10^{24}(m_{\text{Sn}}+4m_{\text{I}})/5N_{\text{A}}$, where m_{Sn} and m_{I} are the atomic weight of the tin and the iodine atoms, respectively, N_{A} is Avogadro number. In Fig. 5, ρ_m is plotted together with the density of the crystalline phases I and III as a function of pressure. As seen in this figure, the amorphous form has reasonable values at pressures between the crystalline phases. A discontinuous increase in density by $\sim 4\%$ is accompanied by the recrystallization at 61 GPa. The data appear to show relatively large deviation during compression in the pressure range of 25–35 GPa. The amorphous structure in this pressure range is expected to be still in a transient state where heavily deformed molecules coexist with denser random-packing arrangement. Such a complex structure will have the distribution of atomic distances much broader than the relatively uniform amorphous structure. This makes it somewhat difficult to choose a proper value of r_{min} used to optimize $G(r)$ and may causes the deviation.

IV. DISCUSSION

The measured $G(r)$'s in the present study show that the tetrahedral SnI_4 molecules no longer exist in the high-

TABLE I. Positions of peaks in $S(Q)$ and in $G(r)$ and the average number density obtained in the amorphous form of SnI_4.

P /GPa	Q_1	Q_2 /Å^{-1}	Q_3	r_1	r_2 /Å	r_3	$Q_1 r_1$	ρ_0 /Å^{-3}
25	2.39	3.91	4.66	3.29	5.56	6.78	7.86	0.0416
30	2.42	3.99	4.74	3.23	5.49	6.49	7.81	0.0427
35	2.45	4.02	4.80	3.14	5.36	6.65	7.69	0.0429
45	2.50	4.16	4.93	3.07	5.23	6.15	7.67	0.0462
54	2.53	4.25	4.98	3.02	5.13	5.98	7.64	0.0485
55	2.55	4.27	5.03	3.02	5.16	6.07	7.70	0.0490

pressure amorphous form above 25 GPa. To confirm this result, we calculated the structure factor of an amorphous model involving the SnI_4 molecule as a structural unit and compared it with the experimentally obtained $S(Q)$. Among three molecular models so far proposed, we chose a dimer model suggested from Raman spectroscopy.[21] The configuration in this model is that two tetrahedral molecules form a dimer in the way that their basal planes face to each other and that the dimers are randomly oriented in the amorphous structure. For the calculation of the structure factor we exploited the procedure developed by Misawa[34,35] for tetrahedral molecular liquids.

In our treatment, the dimer is characterized by the distance R_c between tin atoms forming a pair. The hard-sphere model by Percus-Yevik was applied to calculate the structure factor for the packing of uncorrelated dimers. Two parameters used in their model, the effective diameter of the hard sphere σ and the packing fraction η were estimated to be, respectively, 5.14 Å from a volume of the SnI_4 molecule at 1 atm and 0.59 from the average number density estimated at 25 GPa.

Figure 6 illustrates the experimental $S(Q)$ at 25 GPa and the calculated $S(Q)$s for some different sizes of dimers with R_c=4.0, 3.0, and 2.0 Å together with the measured $S(Q)$ for liquid SnI_4 at 1 atm.[36] As immediately noted in Fig. 6, only $S(Q)$ for the amorphous form is different since all of others have a common feature of oscillation above $Q \sim 5$ Å^{-1} due to the intramolecular interference term. Furthermore, the sharp first peak for the amorphous form cannot be observed in others. Those facts indicate that the tetrahedral SnI_4 molecules are completely dissociated in the amorphous structure above 25 GPa.

Another possible structure model for high-pressure amorphous form is an intermediate structure resulting from an incomplete transformation to a crystalline phase and consisting of disordered, very small crystals of the crystalline phase. In the case of SnI_4, such a crystalline phase could be the crystalline phase III, CP-III. The structure of CP-III is suggested to be analogous to a substitutional binary alloy in which tin and iodine atoms are distributed randomly on the face-centered cubic-lattice sites.[26] Figure 7 illustrates a comparison of the measured $G(r)$ at 55 GPa with the atomic distances in CP-III with the lattice constant a=4.248 Å at 61 GPa.[18] Strong ordering in the amorphous structure can be found at $r \sim 3.0$, 5.2, 6.0, and 7.7 Å and weak ordering at 3.9 Å, but not at r=4.248 Å. This distance in CP-III arises from local octahedral configuration inherent in the fcc structure and, hence, its absence is incompatible with the micro-

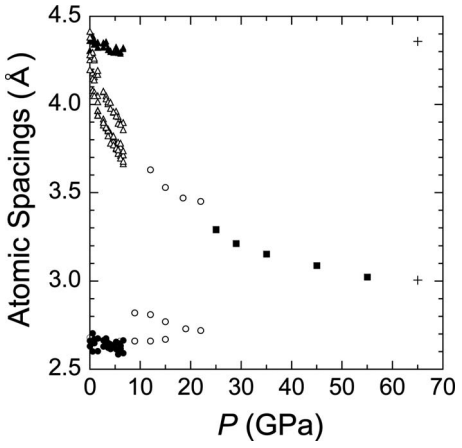

FIG. 4. Atomic spacing in the amorphous form and in the crystalline phases of SnI_4 with increasing pressure; the nearest-neighbor spacing in the amorphous form (closed squares), the spacing measured by XAFS (Ref. 24) (open circles), the first and the second atomic distances in CP-III (crosses), the intramolecular Sn-I distance (closed circles), the intramolecular I-I distance (closed triangles), and the intermolecular I-I distance (open triangles) in CP-I.

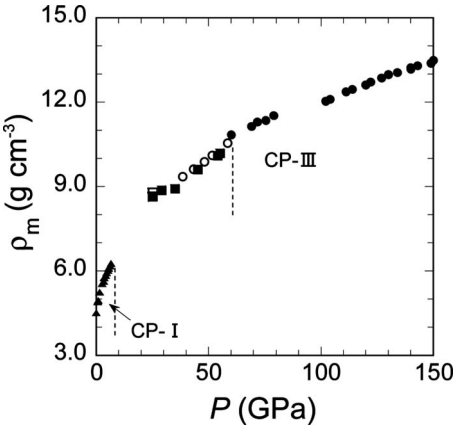

FIG. 5. Density ρ_m of the amorphous form (closed and open squares) and crystalline phases CP-I (closed triangles) and CP-III (closed and open circles) in SnI_4. Closed and open symbols denote the density measured on compression and on decompression, respectively.

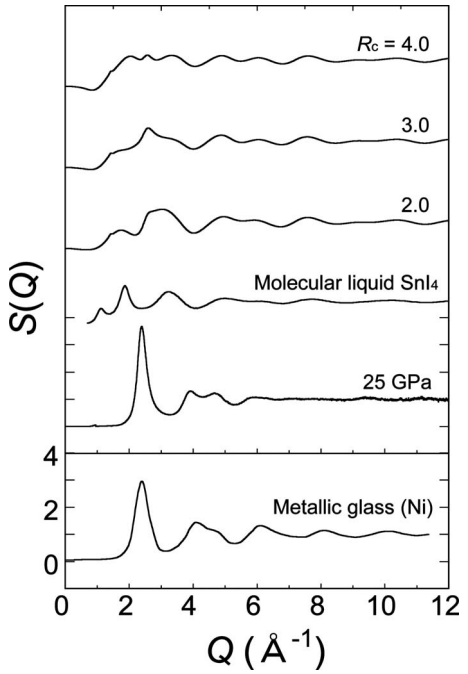

FIG. 6. Comparison of the structure factor $S(Q)$ for amorphous SnI_4 at 25 GPa with that measured in molecular liquid SnI_4 at 1 atm, calculated $S(Q)$ for the dimerized molecules model with various R_c (see text), and experimental one for metallic glass of Ni (Ref. 39). The horizontal scale for $S(Q)$ of Ni glass is changed so as to coincide the position of its first peak with that of the amorphous form.

crystalline picture. Moreover, the calculation of $S(Q)$ for the microcrystalline fcc lattice by Cargill[37,38] demonstrated that all peaks became equally broad and the third peak was stronger in magnitude than the second peak. These features are totally different from those of measured $S(Q)$ for amorphous SnI_4. Thus, we ruled out the possibility that the high-pressure amorphous form of SnI_4 consists of crystallites of the crystalline phase III. It is noteworthy in Fig. 3 that the subsidiary peak at $r \sim 3.9$ Å becomes more distinct with approaching toward the recrystallization pressure of 61 GPa. Although a change in the spacing with pressure is not clearly observed, the formation of the new second-nearest-neighbor bonding

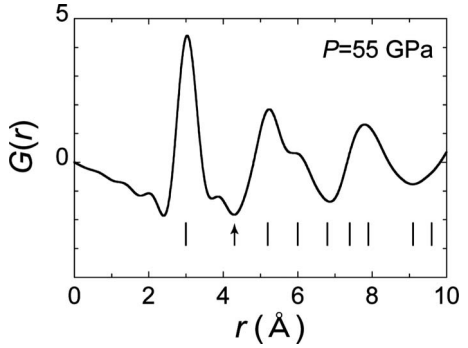

FIG. 7. Comparison the atomic spacing of the amorphous form at 55 GPa (solid line) with that of the crystalline phase III with a =4.248 Å at 61 GPa (bar). Arrow represents the second-nearest-neighbor distance in CP-III.

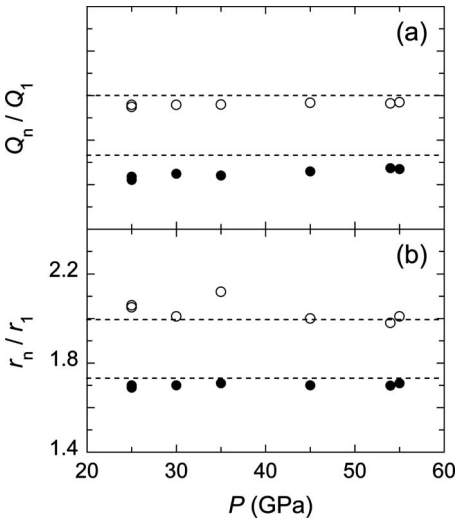

FIG. 8. Positions of the second and third peaks scaled by the first peak in (a) $S(Q)$ and (b) $G(r)$. Broken lines indicate the values derived from the dense random packing of hard-sphere model; (a) $Q_2/Q_1=1.73$ and $Q_3/Q_1=2.00$, (b) $r_2/r_1=1.73$ and $r_3/r_1=1.99$.

could be a precursor of the transformation to the crystalline phase III.

We finally found marked similarities in structure factor between high-pressure amorphous SnI_4 and elemental metallic glasses of Ni and Fe,[39] as shown in Fig. 6. Common basic features are the sharp main peak and the splitting of the second peak. They have been well reproduced by the dense random packing of hard-spheres (DRPHS) model,[38,40–42] though the observation that the second peak is higher in magnitude than the third peak is better demonstrated by either the dense random packing of compressible soft-spheres model (DRPSS)[43,44] or the relaxed Bernal model[45] than the DPRHS model. To see the capability of these models to describe the structure of amorphous SnI_4, we examined the positions of peaks in the structure factor scaled by the wave number of the first peak Q_1. The structure factor for the DRPHS model has the second peak at $Q_2/Q_1 \sim 1.73$ and the third peak at $Q_3/Q_1 \sim 2.00$.[38,42] The present data plotted in Fig. 8(a) show that amorphous SnI_4 takes the values of Q_2/Q_1 and Q_3/Q_1 very close to those specific values of the DRPHS model even at low pressures and both peaks approach to these values with increasing pressure. We also examined the positions of peaks scaled by the shortest spacing r_1 in the corresponding radial distribution function. Calculation of $G(r)$ for a dense random packing of several thousands hard spheres by Finney[41] demonstrated that the second and third peaks have maxima at $r_2/r_1 \sim 1.73$ and $r_3/r_1 \sim 1.99$, respectively. The present results plotted in Fig. 8(b) are in good agreement with the Finney's results. These facts suggest that the structure of high-pressure amorphous SnI_4 can be approximated by the assemblage derived from random packing of equal-sized spheres. Since the atomic number of iodine differs only by two from that of tin and amorphous SnI_4 is in a metallic state above 12 GPa,[23] we may presume these atoms to be not much different in size at high pressures.

The coordination number n was estimated from the area of the first peak using relations (4) and (5),

$$n = 2\int_0^{r_{\max}} 4\pi r^2 \rho(r) dr, \tag{4}$$

$$4\pi r^2 \rho(r) = rG(r) + 4\pi r^2 \rho_0, \tag{5}$$

where $r_{\max}$ is the maximum of the first peak in the $4\pi r^2\rho(r)$ curve. In this calculation, SnI_4 was assumed to be a one-component system because of little difference in atomic scattering factor between tin and iodine. The evaluation yielded almost constant coordination number of $n \sim 10$ between 35 and 55 GPa. This value lies within a range of 7–12 derived from various DRPHS and DRPSS models. An anomalously large value of 13 was estimated at 25 GPa. This seems to be attributed to double counting of the area of the peak corresponding to the elongated Sn-I distance which is located at $r \sim 2.6$ Å in the lower side of the first peak in $G(r)$ and, hence, this result may be discarded. It is well known that in the assemblage based on the dense random-packing model Bernal's polygons consisting of tetrahedra or slightly deformed tetrahedra are irregularly and continuously arranged.[44] We believe that the high-pressure amorphous form of SnI_4 has a similar structure, in which the most basic structural unit is a tetrahedron composed of four iodine and substitutional tin atoms but not the pentaatomic tetrahedral SnI_4 molecule.

It is of interest to compare structural properties of high-pressure amorphous SnI_4 with other amorphous systems, in particular, showing polyamorphism under pressure. Price *et al.*[46] has suggested that $Q_1 r_1$ and $Q_1 d_s$, where d_s is the mean atomic spacing $d_s^3 = \rho_0 \pi / 6$, are useful quantities to observe similarities in intermediate range order between different types of disordered systems. Using a similar plot of $Q_1 r_1$ and d_s / r_1, for tetrahedral low-density, high-density, and very high-density glass and liquid forms of H_2O, Ge, and Si, Benmore *et al.*[12] has shown that there is a general trend with increasing density that progressively approaches the well-known Ehrenfest limit for a dense random packing of hard spheres, $Q_1 r_1 \cong 5\pi/2 \sim 7.85$.[46] As seen in Table I, the first peak in the high-pressure amorphous form of SnI_4 agrees with this limit. If SnI_4 is the system following the general trend described above, it could be expected that the transformation to the low-density amorphous form might occur at lower pressure. Figure 9 shows our preliminary data of $S(Q)$ and $G(r)$ measured at 1.1 GPa after decompression of the high-pressure amorphous form. The nearest- and the next-nearest-neighbor distances determined from $G(r)$ precisely agree with the Sn-I and the I-I intramolecular distances, respectively. The values of $Q_1 r_1$ and d_s / r_1 were 4.96 and 1.61, respectively. Those observations suggest the molecular character of the low-pressure amorphous form and the occurrence of drastic modification of the amorphous structure involving the change in electronic configurations. The details of pressure evolution of the amorphous structure will be discussed elsewhere.

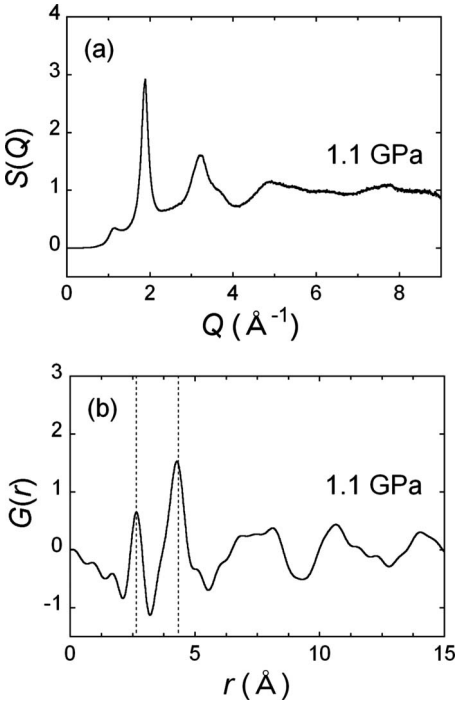

FIG. 9. (a) Structure factor and (b) reduced radial distribution function for the molecular amorphous at 1.1 GPa. Two broken lines shown in (b) denote the intramolecular bond distances of $r_{\text{Sn-I}} = 2.65$ Å and $r_{\text{I-I}} = 4.33$ Å.

V. SUMMARY

We performed the synchrotron-radiation x-ray diffraction measurement for the structural analysis of the pressure-induced amorphous form of SnI_4 up to 60 GPa at room temperature. The structure factor $S(Q)$, the reduced radial distribution function $G(r)$ and the density are obtained at 25, 30, 35, 45, 54, and 55 GPa. The experimentally obtained $G(r)$ has provided the direct evidence for the absence of the tetrahedral SnI_4 molecules in the amorphous form. Characteristic features of measured $S(Q)$ and $G(r)$ are in quantitative agreement with those derived from the dense random packing of hard-spheres model.

ACKNOWLEDGMENTS

The authors are grateful to S. Kohara for useful discussion about the structural analysis of the noncrystalline materials. Part of this work was performed at SPring-8 under the approval of the Japan Synchrotron Radiation Research Institute (Proposals No. 2000A0056ND and No. 2000B0381ND). This work was supported by a Grant-in-Aid for Scientific Research from the Ministry of Education, Culture, Sports, Science and Technology, Japan (Grant No. 12640309).

*Present address: Center for Transdisciplinary Research, Niigata University, 8050 Ikarashi-Ninocho, Nishi-ku, Niigata, Niigata 950-2181, Japan; ohmura@phys.sc.niigata-u.ac.jp

†Present address: Advanced Manufacturing Research Institute, National Institute of Advanced Industrial Science and Technology, 2266 Anagahora, Shimo-Shidami, Moriyama-ku, Nagoya, Aichi 463-8560, Japan.

[1] O. Mishima, L. D. Calvert, and E. Whalley, Nature (London) **310**, 393 (1984).
[2] O. Mishima, Nature (London) **384**, 546 (1996).
[3] R. J. Hemley, A. P. Jephcoat, H. K. Mao, L. C. Ming, and M. H. Manghnani, Nature (London) **334**, 52 (1988).
[4] Q. Williams and R. Jeanloz, Nature (London) **338**, 413 (1989).
[5] H. Luo and A. L. Ruoff, Phys. Rev. B **48**, 569 (1993).
[6] E. Gregoryanz, A. F. Goncharov, R. J. Hemley, and H. K. Mao, Phys. Rev. B **64**, 052103 (2001).
[7] M. P. Pasternak, R. D. Taylor, M. B. Kruger, R. Jeanloz, J.-P. Itie, and A. Polian, Phys. Rev. Lett. **72**, 2733 (1994).
[8] W. Williamson and S. A. Lee, Phys. Rev. B **44**, 9853 (1991).
[9] G. Yu. Machavariani, G. Kh. Rozenberg, M. P. Pasternak, O. Naaman, and R. D. Taylor, Physica B (Amsterdam) **265**, 105 (1999).
[10] M. B. Kruger and C. Meade, Phys. Rev. B **55**, 1 (1997).
[11] O. Mishima, L. D. Calvert, and E. Whalley, Nature (London) **314**, 76 (1985).
[12] C. J. Benmore, R. T. Hart, Q. Mei, D. L. Price, J. Yarger, C. A. Tulk, and D. D. Klug, Phys. Rev. B **72**, 132201 (2005).
[13] V. V. Brazhkin, E. L. Gromnitskaya, O. V. Stal'gorova, and A. G. Lyapin, Rev. High Pressure Sci. Technol. **7**, 1129 (1998).
[14] C. Meade, R. J. Hemley, and H. K. Mao, Phys. Rev. Lett. **69**, 1387 (1992).
[15] J. P. Itie, A. Polian, G. Calas, J. Petiau, A. Fontaine, and H. Tolentino, Phys. Rev. Lett. **63**, 398 (1989).
[16] Y. Katayama, T. Mizutani, W. Utsumi, O. Shimomura, M. Yamanaka, and K. Funakoshi, Nature (London) **403**, 170 (2000).
[17] T. Morishita, Phys. Rev. Lett. **87**, 105701 (2001).
[18] N. Hamaya, K. Sato, K. Usui-Watanabe, K. Fuchizaki, Y. Fujii, and Y. Ohishi, Phys. Rev. Lett. **79**, 4597 (1997).
[19] B. M. Riggleman and H. G. Drickamer, J. Chem. Phys. **38**, 2721 (1963).
[20] Y. Fujii, M. Kowaka, and A. Onodera, J. Phys. C **18**, 789 (1985).
[21] S. Sugai, J. Phys. C **18**, 799 (1985).
[22] M. Pasternak and R. D. Taylor, Phys. Rev. B **37**, 8130 (1988).
[23] A. L. Chen, P. Y. Yu, and M. P. Pasternak, Phys. Rev. B **44**, 2883 (1991).
[24] F. Wang and R. Ingalls, in *High Pressure Science and Technology*, edited by W. A. Trzeciakowski (World Scientific, Singapore, 1996), p. 289.
[25] N. Takeshita, S. Kometani, K. Shimizu, K. Amaya, N. Hamaya, and S. Endo, J. Phys. Soc. Jpn. **65**, 3400 (1996).
[26] K. Sato, Ph.D. thesis, Ochanomizu University, 2000.
[27] A. Ohmura, N. Hamaya, K. Sato, C. Ogawa, M. Isshiki, and Y. Ohishi, J. Phys.: Condens. Matter **14**, 10553 (2002).
[28] H. K. Mao, P. M. Bell, J. W. Shaner, and D. J. Steinberg, J. Appl. Phys. **49**, 3276 (1978).
[29] J. Krogh-Moe, Acta Crystallogr. **9**, 951 (1956).
[30] N. Norman, Acta Crystallogr. **10**, 370 (1957).
[31] T. E. Faber and J. Ziman, Philos. Mag. **11**, 153 (1965).
[32] R. Kaplow, S. L. Strong, and B. L. Averbach, Phys. Rev. **138**, A1336 (1965).
[33] J. H. Eggert, G. Weck, P. Loubeyre, and M. Mezouar, Phys. Rev. B **65**, 174105 (2002).
[34] M. Misawa, J. Chem. Phys. **91**, 5648 (1989).
[35] M. Misawa, J. Chem. Phys. **93**, 6774 (1990).
[36] K. Fuchizaki, S. Kohara, Y. Ohishi, and N. Hamaya, J. Chem. Phys. **127**, 064504 (2007).
[37] G. S. Cargill, J. Appl. Phys. **41**, 12 (1970).
[38] G. S. Cargill III, Solid State Phys. **30**, 227 (1975).
[39] T. Ichikawa, Phys. Status Solidi A **19**, 707 (1973).
[40] J. D. Bernal, Nature (London) **183**, 141 (1959).
[41] J. L. Finney, Proc. R. Soc. London, Ser. A **319**, 479 (1970).
[42] T. Ichikawa, Phys. Status Solidi A **29**, 293 (1975).
[43] G. A. N. Connell, Solid State Commun. **16**, 109 (1975).
[44] J. L. Finney and J. Wallace, J. Non-Cryst. Solids **43**, 165 (1981).
[45] J. A. Barker, M. R. Hoare, and J. L. Finney, Nature (London) **257**, 120 (1975).
[46] D. L. Price, S. C. Moss, R. Reijers, M.-L. Saboungi, and S. Susman, J. Phys.: Condens. Matter **1**, 1005 (1989).